Supplement of Biogeosciences, 18, 2465–2485, 2021
https://doi.org/10.5194/bg-18-2465-2021-supplement

Biogeosciences Open Access EGU

Supplement of

Anthropocene climate warming enhances autochthonous carbon cycling in an upland Arctic lake, Disko Island, West Greenland

Mark A. Stevenson et al.

Correspondence to: Mark A. Stevenson (mark.stevenson@newcastle.ac.uk)

Table S1 Detailed vegetation composition surveys of the three study lakes local catchments, which form vegetation survey derived estimations of ground cover in Table 1.

	Disko 2 (%)	**Disko 1 (%)**	**Disko 4 (%)**
Total moss/lichen	**27.3**	**37.5**	**37.0**
White moss		15.3	
Grey moss		3.7	
Green moss	1.3	12.2	7.9
Dead/decaying moss	1.2	3.6	
Long green moss		2.1	
Yellow moss	13.7	0.6	2.3
Cetraria nivalis lichen	6.8		3.2
Cladonia arbuscular lichen			5.2
Umbilicaria-type lichen	3.5		2.0
White lichen	0.7		16.4
Total plants	**19.2**	**32.7**	**44.4**
Salix arctica	5.3	5.2	8.9
Salix arctica seedling	6.0	11.0	14.0
Poaceae	1.6	5.1	2.1
Dead leaves/branches	0.7	2.4	2.2
Carex		5.8	4.7
Eriophorum spp.		0.4	
Saxifraga	4.8	2.8	10.1
Plant roots	0.6		
Chamerion latifolium			2.4
Total bare ground	**53.5**	**29.8**	**18.6**
Guano		3.0	0.1
Bare organic soil		10.8	13.2
Bare rock/gravel	53.5	16.1	5.2
No. 10x10m plots	3	5	3
No. of 1x1m quadrats	15	25	15

All values are percentages derived as estimated mean values per study catchment from repeated randomised quadrat surveys of the lower catchments (N=5) within each 10 x 10 m study area (N=3 to 5). Locations of study plots are indicated in lake catchment maps A-E (Disko 1) and A-C (Disko 2 & 4).

Table S2 Descriptions of lipid (*n*-alkane, *n*-alkanol and *n*-alkanoic acid) histograms from Fig. 5.

Sample	a) *n*-alkanes	b) *n*-alkanols	c) *n*-alkanoic acids
Algal benthic rock scrape	Unimodal around *n*-C_{23}. Odd predominant.	Unimodal around *n*-C_{26}, followed by *n*-C_{24}. Even predominance.	Dominant in *n*-C_{16}, with slight contributions in *n*-C_{14}, *n*-C_{18} & *n*-C_{24}. Even predominance.
Potamogeton sp.	Highest *n*-C_{31}. Mostly odd predominant.	Dominant *n*-C_{22} followed by secondary *n*-C_{18}. Even predominance.	Dominant *n*-C_{16}, minor peak in *n*-C_{14}. Even predominant.
Green moss	Highest *n*-C_{31}. Odd predominant.	Unimodal around *n*-C_{26}. Even predominant.	Bimodal around *n*-C_{16} and *n*-C_{24}. Even predominant.
Black moss	Highest *n*-C_{25}. Generally odd predominant.	Dominant *n*-C_{18} followed by *n*-C_{26}. Even predominant.	Dominant in *n*-C_{16} with a secondary minor peak in *n*-C_{18}. Even predominant.
Chamerion latifolium	Unimodal around odd *n*-C_{25} followed by *n*-C_{27}. Odd predominant.	Unimodal around *n*-C_{24}, followed by *n*-C_{22}. Even predominant.	Dominant in *n*-C_{16} with scondary *n*-C_{26}. Even predominant.
***Harrimanella hypnoides* (1)**	Unimodal around *n*-C_{31}, followed by *n*-C_{29}. Odd predominant.	Unimodal around *n*-C_{26}, followed by *n*-C_{28}. Even predominant.	Dominant in *n*-C_{18} followed by *n*-C_{16}. Even predominant.
***Harrimanella hypnoides* (2)**	Unimodal around *n*-C_{29}, followed by *n*-C_{31}. Odd predominant.	Dominant *n*-C_{22}. Even predominant.	Dominant in *n*-C_{16}. Even predominant.
Herbaceous plant	Unimodal *n*-C_{29}. Odd predominant.	Unimodal around *n*-C_{22}. Even predominant.	Bimodal with *n*-C_{22}, and smaller *n*-C_{20} dominant, followed by *n*-C_{16}. Even predominant.
***Salix arctica* (leaf)**	Unimodal around *n*-C_{27} followed by *n*-C_{25}. Odd predominant.	Unimodal around *n*-C_{24}, followed by *n*-C_{22}. Even predominant.	Dominant in *n*-C_{16} with smaller *n*-C_{24}. Mostly even predominant.
PLOT C - Soil	Highest peak *n*-C_{29} but very mixed distribution across full range. Only very slightly odd predominant.	Bimodal but dominant in *n*-C_{18} with further contributions in *n*-C_{22}, *n*-C_{24}, *n*-C_{26} & *n*-C_{28}. Even predominant.	Dominant in *n*-C_{16}, followed by *n*-C_{18}. Secondary minor peak around *n*-C_{24}. Even predominant.
Catchment summit - Soil	Unimodal around *n*-C_{31} followed by *n*-C_{29}. Odd predominant.	Highest in *n*-C_{22}, *n*-C_{24}, *n*-C_{26}. Even predominant.	Dominant in *n*-C_{16}, followed by *n*-C_{18}. Even predominant.
Surface sediment	Dominant *n*-C_{21} with secondary *n*-C_{31} maximum. Slight odd predominance & extended range.	Bi-modal distribution reflecting mixed inputs with peaks in *n*-C_{16} and *n*-C_{22}.	Dominant in *n*-C_{16}. Mostly even predominant.

Table S3 Interpretation of lipid ratios in the Disko 2 catchment-lake system from Table 4.

Ratio	Interpretation	Evidenced by?
***n*-alkanes**		
CPI 2 (Carbon Preference Index 2) (Marzi *et al.*, 1993) derived from (Bray & Evans, 1961).	Good indicator of terrestrial plants including woody and herbaceous varieties.	Higher values in *Salix arctica* (18.5), unidentified herbaceous plant (25.9) and *Harrimanella hypnoides* (39.6 – 27.6). Low values in catchment (5.2) and Plot C (1.3) soil samples and surface sediment (2.4).
TAR_{HC} (Terrestrial and aquatic hydrocarbon ratio) (Bourbonniere & Meyers, 1996)	Excellent indicator of leafy vascular plants.	High values in ericaceous shrub *Harrimanella hypnoides* (18,899.2 – 2,980.3) and the unidentified herbaceous plant (1,523.1). Lower ratios for black moss (3.0), green moss (8.0) and the algal benthic rock scrape (6.2). Catchment soil with visible rootlets was higher (357.7) than Plot C soil (18.9) or surface sediment (5.1).
P_{WAX} (Zheng *et al.*, 2007)	Good indicator of multiple terrestrial inputs.	Slightly higher values in herbaceous plants, *Harrimanella hypnoides* (1.2-1.0), the unidentified herbaceous plant (1.1.). Both soil samples were > 1. Lowest values in algal benthic rock scrape (<0.5).
The *n*-C_{27} to total saturated *n*-alkanes ratio	Good indicator of some plants.	Highest values in the *Salix arctica* (leaf) sample (26.0) and Chamerion latifolium (26.0), with lowest values in the algal benthic rock scrape (7.7) and surface sediment.
***n*-alkanoic acids**		
CPI_T ratio (Carbon Preference Index for total *n*-alkanoic acids) (Matsuda & Koyama, 1977b)	Good indicator of aquatic macrophyte and moss contributions.	High values in aquatic macrophyte *Potamogeton sp.* (74.3), and black moss samples (69.7). Low in both soils (15.1 - 11.7).
n-C_{30} to total saturated *n*-alkanoic acids	Good indicator of some non-woody herbaceous terrestrial inputs.	High in *Harrimanella hypnoides* (sample 2) (4.2) and some soil samples (Plot C soil 2.0) but was lower in the catchment soil sample (0.2), highlighting localised variations in patchy soils. Lowest values were in moss samples (0-0.1), the algal benthic rock scrape (0.0) and surface sediment (0.1).
***n*-alkanols**		
n-C_{16}: total saturated *n*-alkanols	Good indicator of aquatic macrophytes.	High in *Potamogeton sp.* (12.4), black moss (8.2) and catchment soils (Plot C soil sample 4.9).
n-C_{24}: total saturated *n*-alkanols	Good indicator of more woody terrestrial plants.	High in more woody terrestrial plants such as *Salix arctia* (42.2) and secondary contributions in green moss (26.2).
Sterols		
Brassicasterol/ total sterols	Clear indicator of algae and moss	High in the algal benthic rock scrape (57.8) and black moss (56.6), but low in *Salix arctica* (0.4). Surface sediment was extremely high in this ratio (608.7).

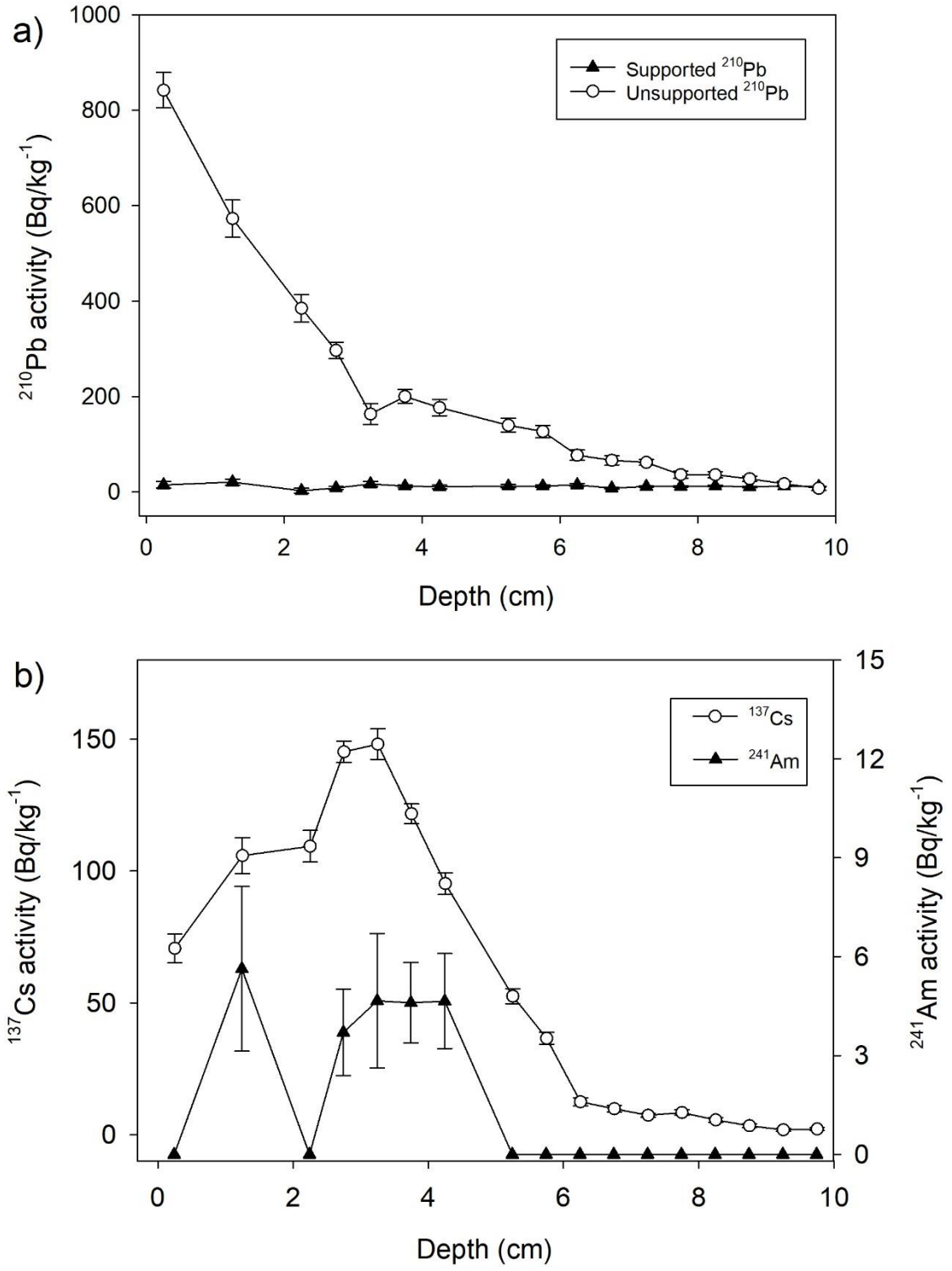

Fig. S1: a) ^{210}Pb supported and unsupported activity plotted against core depth. **b)** ^{137}Cs and ^{241}Am activity plotted against core depth. Standard errors (1σ) calculated from counting statistics.

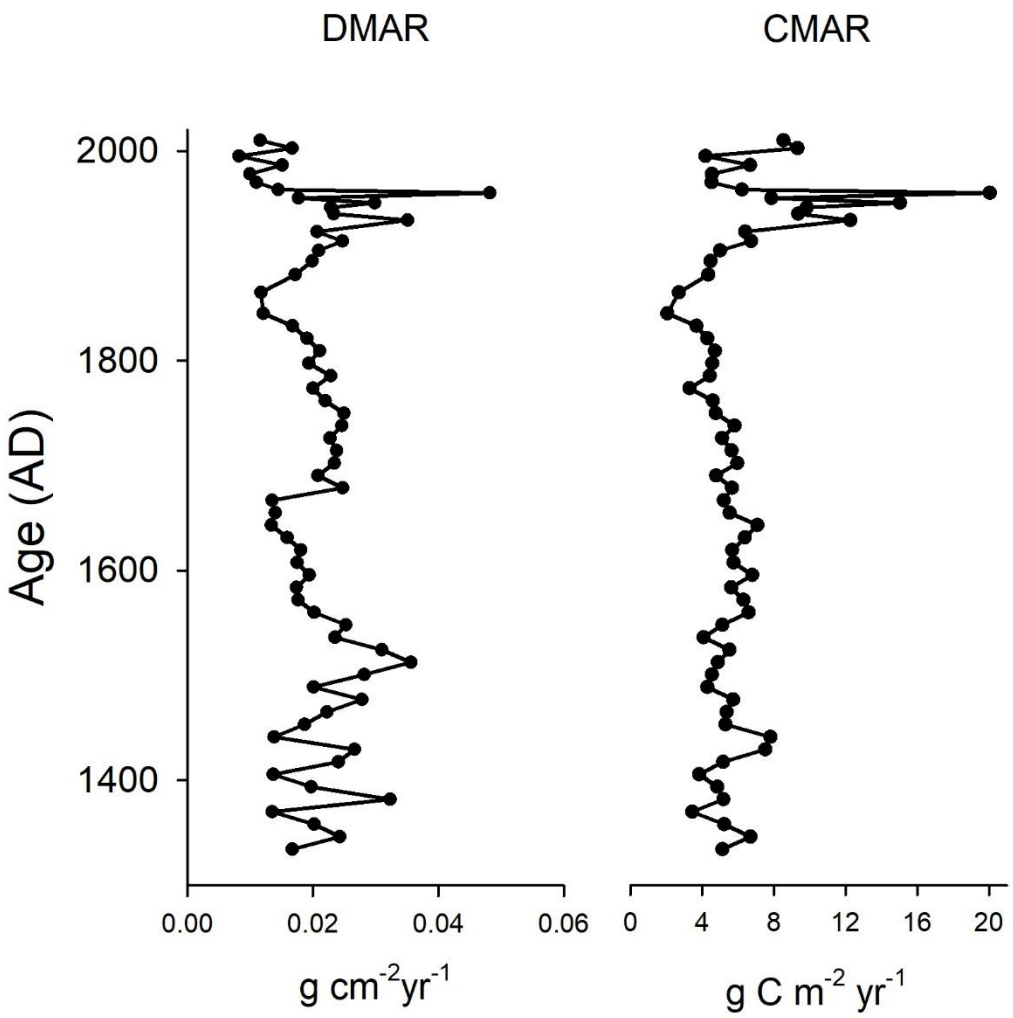

Fig. S2: Dry mass accumulation rate (DMAR, in g cm^{-2} yr^{-1}) and carbon mass accumulation rate (CMAR, in g C $m^{-}2$ yr^{-1}) plotted against age (AD).

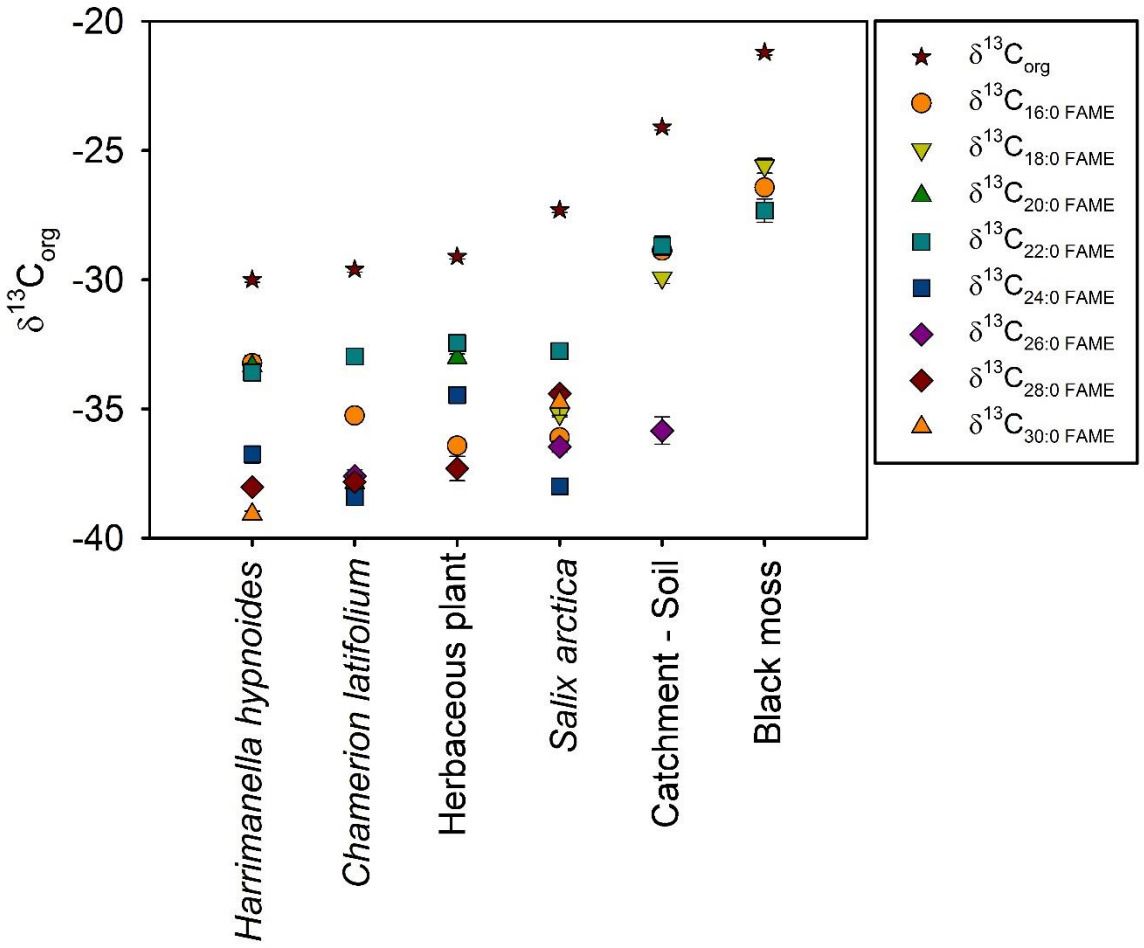

Fig. S3: Bulk $\delta^{13}C_{org}$ compared with compound-specific $\delta^{13}C_{FAMEs}$ for six selected samples from Disko 2.

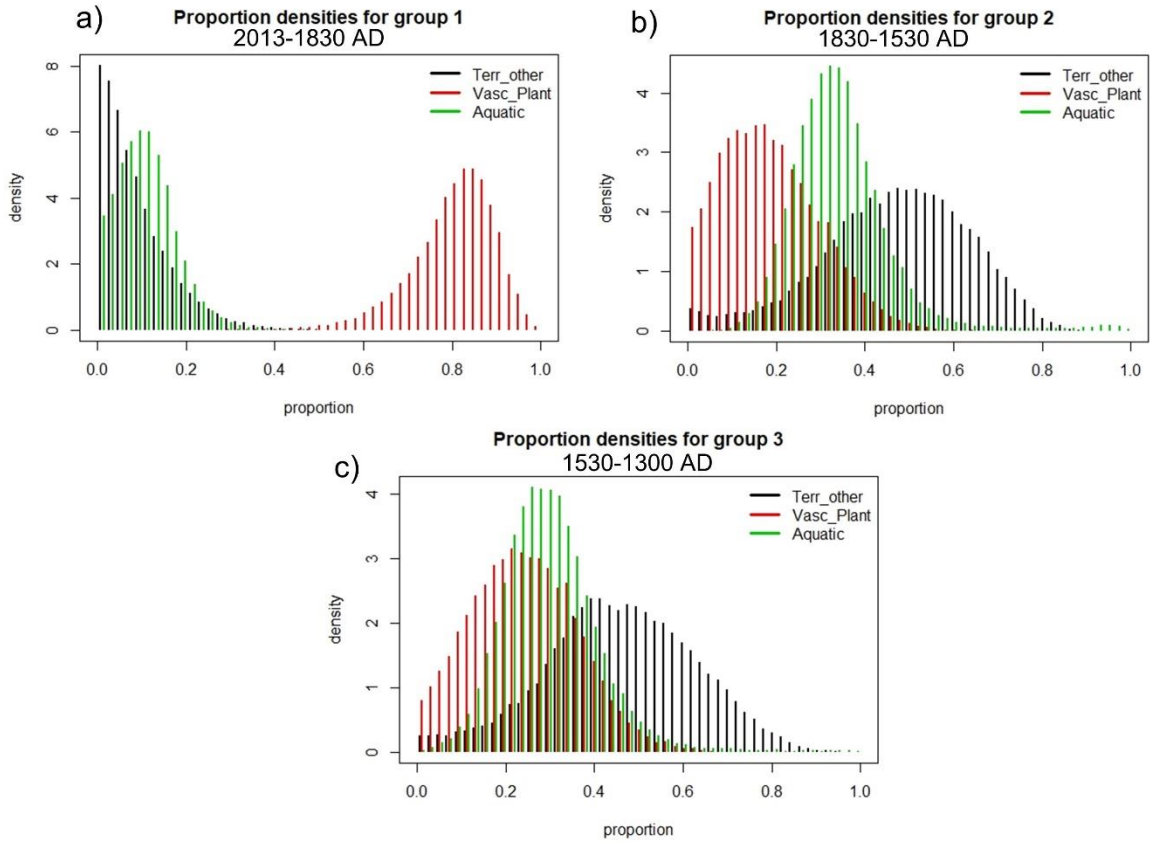

Fig. S4: Population histograms produced in SIAR for **a)** group 1 (2013-1830 AD), **b)** group 2 (1830-1530 AD) and **c)** group 3 (1530-1300 AD). Groups reflect zones A-C indicated in Fig. 7. Each histogram is separated into the three broad catchment sample groups of $\delta^{13}C_{org}$ and C_{org}:N ratio identified in Figure 4 and the model was run against core sediment $\delta^{13}C_{org}$ and C_{org}:N ratio from Disko 2.

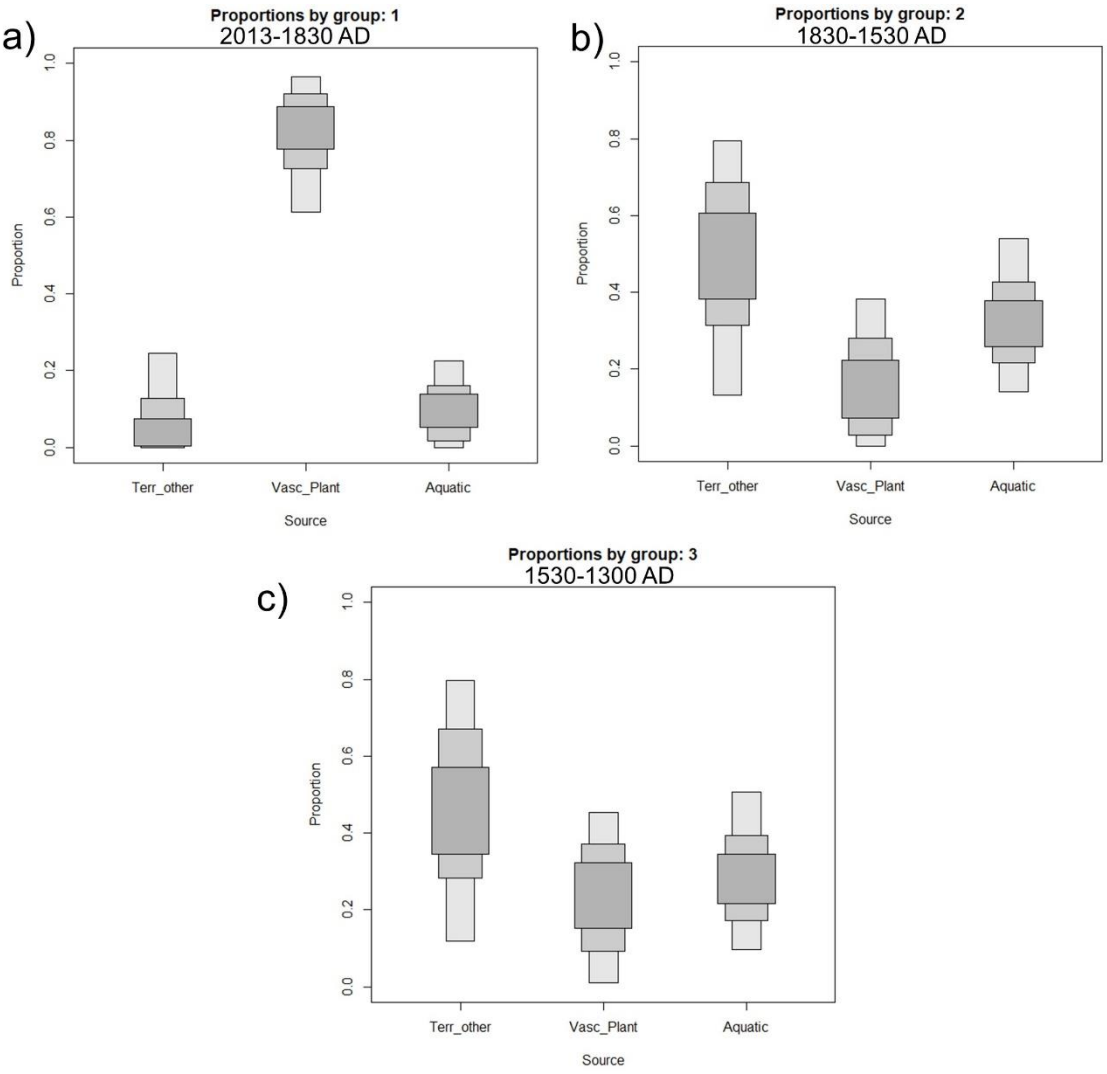

Fig. S5: Proportional boxplot produced in SIAR for **a)** group 1 (2013-1830 AD), **b)** group 2 (1830-1530 AD) and **c)** group 3 (1530-1300 AD). Groups reflect zones A-C indicated in Fig. 7. Each boxplot is separated into the three broad catchment sample groups of $\delta^{13}C_{org}$ and C_{org}:N ratio identified in Figure 4 and the model was run against core sediment $\delta^{13}C_{org}$ and C_{org}:N ratio from Disko 2.

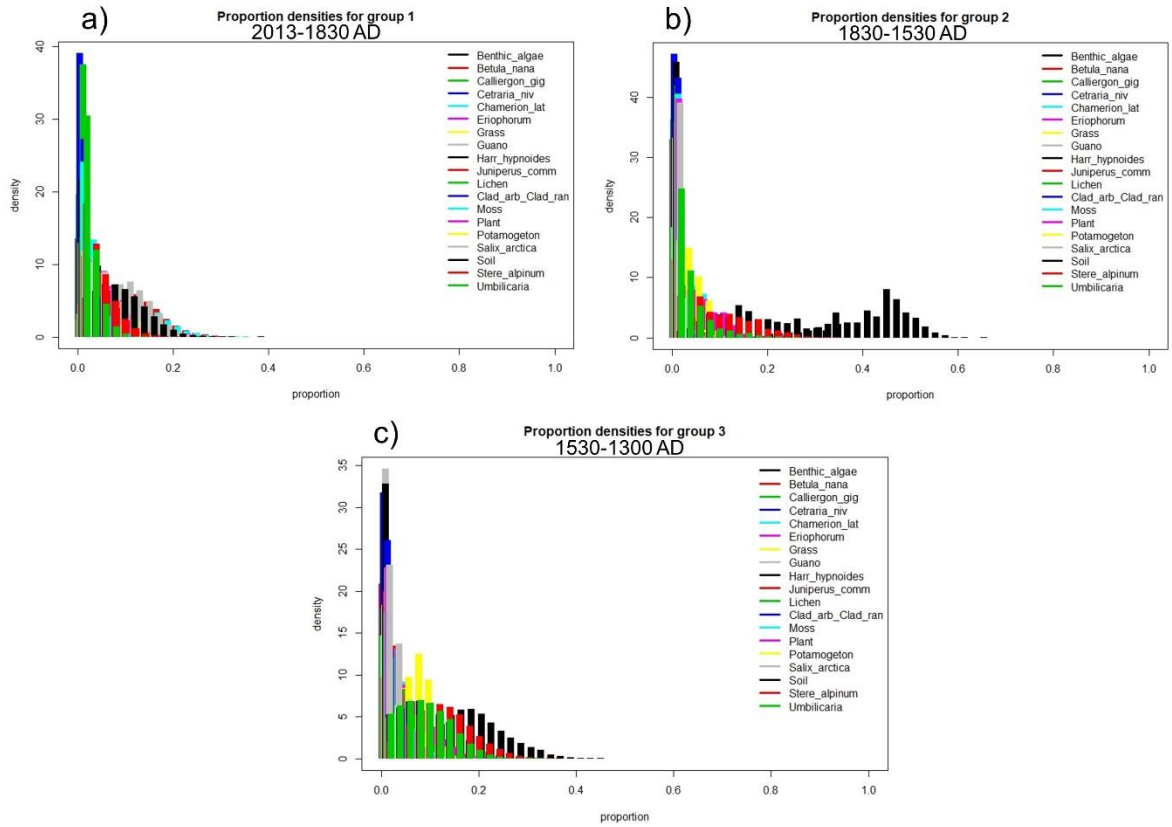

Fig. S6: Population histograms produced in SIAR for **a)** group 1 (2013-1830 AD), **b)** group 2 (1830-1530 AD) and **c)** group 3 (1530-1300 AD). Groups reflect zones A-C indicated in Fig. 7. Each histogram is separated into the nineteen specific species level groups of $\delta^{13}C_{org}$ and C_{org}:N ratio identified in Figure 4 and the model was run against core sediment $\delta^{13}C_{org}$ and C_{org}:N ratio from Disko 2.

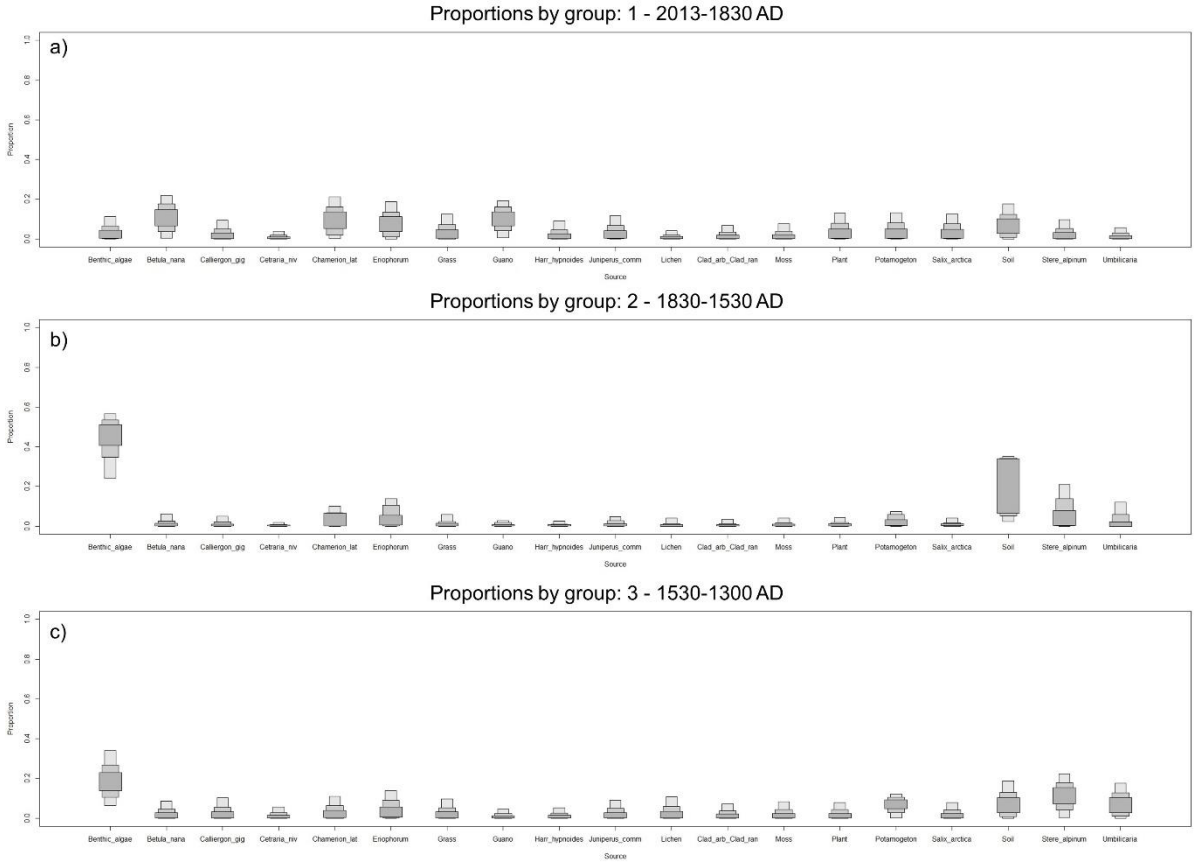

Fig. S7: Proportional boxplots produced in SIAR for **a)** group 1 (2013-1830 AD), **b)** group 2 (1830-1530 AD) and **c)** group 3 (1530-1300 AD). Groups reflect zones A-C indicated in Fig. 7. Each boxplot is separated into the nineteen specific species level groups of $\delta^{13}C_{org}$ and C_{org}:N ratio identified in Figure 4 and the model was run against core sediment $\delta^{13}C_{org}$ and C_{org}:N ratio from Disko 2.